

Effect of Alkaline Peroxide Pre-treatment on Microfibrillated Cellulose from Oil Palm Fronds Rachis Amenable for Pulp and Paper and Bio-composite Production

Abdul Wahab Taiwo Owolabi,^{a,b*} Ghazali Arniza,^a Wanrosli wan Daud,^a and Abbas F. M. Alkharkhi^a

Effects of alkaline peroxide (AP) pre-treatment were investigated with respect to the extracted cellulose fibres from the vascular bundles of oil palm (*Elaeis guineensis*) fronds (OPF) rachis at different AP concentrations. The extracted fibres were prepared through the mechanical fibrillation resulting from the AP pre-treatment concentrations of the rachis. The cellulose fibres obtained were characterized using microscopic (SEM), spectroscopic (FTIR), thermal (TGA-DTG), and X-ray diffraction (XRD) techniques. The screen pulp yield was between 38.07% and 42.69%, which increased with the increase in the AP concentrations. The SEM showed a significant separation of the fibres after the AP pretreatment. FTIR spectroscopy and TGA showed significant dissolution of both lignin and hemicellulose molecules from the treated biomass at higher alkaline peroxide concentrations. The thermal stability of the extracted fibres ranged from 366 °C to 392 °C while the XRD results showed that the cellulose fibre extracted at H₂O₂/NaOH ratio of 2.5%: 2.0%,w/v AP concentrations gave the highest percentage crystallinity (35.7%). The handsheet made from the cellulose fibre showed that tensile, burst, and tear indexes increased with an increase in AP concentration. Duncan Multiple Range Test shows that mild alkaline peroxide pretreatment (medium concentrations) is best favoured for paper making pulp and bio-composite production.

Keywords: Cellulose fibre; Oil palm frond rachis; Vascular bundles; Micro-fibrillated celluloses; DMRT; TGA; FTIR; XRD

Contact information: a: Bioresources and Paper Coating Technology; Universiti Sains Malaysia, Penang; b: Federal Institute of Industrial Research Oshodi, Lagos Nigeria;

* Corresponding author: fathok2375@gmail.com

INTRODUCTION

Since Malaysia is the second largest producer of oil palm (*Elaeis guineensis* Jacq.) in the world, oil palm plantations have become the most important agricultural crop in Malaysia and have constituted the key national economic expansion (Awalludin *et al.* 2015). From the oil palm production activities, palm oil products constitute just 10% of the products, while the remaining 90% remains waste biomass (Ng *et al.* 2015). The rapid expansion of the oil palm plantations throughout Malaysia may likely pose threats to the conservation of native biodiversity. The influence of oil palm expansion on tropical biodiversity has received increasing attention, and several recent reviews have been published. The wastes, which include oil palm trunk OPT that are generated by a 25-year re-plantation scheme, the empty fruit bunches (EFB) that are generated from the palm oil

factory every day, and oil palm fronds (OPF) also generated from every tree pruned once a month are either burnt (as the main energy source for power generation in oil palm mills) or used as organic fertilizer for natural decomposition. Also, EFB is also used in soil mulching as an organic nutrient to reduce the input of inorganic fertiliser (Daud *et al.* 2011; Wanrosli *et al.* 2011; Haafiz *et al.* 2013). OPF is the largest waste generated from oil palm plantations that are yet to attract economic advantages in Malaysia (Wanrosli *et al.* 2007). This situation directly leads to environmental menace causing damage to the land and the surrounding area in which it was dumped. Due to the problems associated with the waste management, commercial use for the waste has been suggested.

Cellulose productions from waste biomass involve removal or dissolution of lignin and extraction of hemicellulose. The source of the original cellulose (Neto *et al.* 2013; Silvério *et al.* 2013) and the type of treatment on the lignocelluloses biomass dictates the quality of the nano-material obtainable cellulose. Different kinds of procedures have been reported on cellulose production. All these methods are characterised by various advantages and disadvantages related to the quantity and quality of cellulose (Kwon *et al.* 2014; Borchani *et al.* 2015). Factors that influence the cellulosic fibres properties include physicochemical composition, mechanical character, which is a measure of the cellulose crystallinity (Ju *et al.* 2015), and fibre morphology, which differs with different plants, cellulose type, and different plant parts (Fahma *et al.* 2011; Khalil *et al.* 2015). Research studies of the correlations between the effect of shapes and sizes of cellulose microfibrils on the cellulose crystallinity parameters have been established (French and Cintrón 2013; Avolio *et al.* 2015). This study was targeted at establishing a relationship between the microscopic structure and powder diffraction pattern and the cellulose crystallinity parameters of cellulose crystal samples (Zhang *et al.* 2015; Ju *et al.* 2015; Li *et al.* 2015b).

The use of alkaline peroxide for cellulose extraction was first reported by Gould (1984) and has been widely used as lignocelluloses biomass pretreatment before the hydrolysis of soluble polysaccharides to form simple sugars. The possible use of alkaline peroxide for pulp and paper production from EFB was recently reported (Ghazali *et al.* 2014). However, the reports did not characterise the fibre formed to establish the fundamental quality of the cellulose fibre. To maximise the use of OPF vascular bundles as biodegradable green composite material, there is a need to explore the natural reinforcement properties, such as thermal stability, chemical composition, crystallinity index, *etc.* However, characterization of alkaline peroxide extracted OPF vascular bundles fibres on pulp and paper and natural reinforcement properties has not been extensively carried out or reported.

The present study characterises the effect of alkaline peroxide at different concentrations on the extracted cellulose fibre from the rachis of oil palm fronds vascular bundles. This research work is aimed at investigating fundamental properties of the OPF vascular bundle fibres to enhance its reinforcement and pulp and paper production. The transformation of the treated fibre on appearance and disappearance of functional groups was evaluated using Fourier transform infrared spectroscopy (FTIR) and the thermal stability of the AP fibres were characterised using thermogravimetric analysis (TGA). The morphology of the fibres was determined by X-ray diffraction XRD analysis and scanning electron micrographs SEM and their morphological features were studied about their application in pulp and paper production and fibres reinforced-polymer composites.

EXPERIMENTAL

Materials

The decorticated oil palm fronds rachis (OPF) was supplied from oil palm plantation Penang. The fibres from rachis were extracted through field retting of the decorticated fronds. The retted fibres were left to dry, shredded, milled, and screened to 500 µm size and kept in plastic bags. All the reagents used for the chemical analysis were of analytical grade.

Methods

Cellulose extraction and handsheet making

The cellulose fibre was isolated from the OPF rachis vascular bundles using a modified method described by Ghazali *et al.* (2014) based on original procedures described by Gould (1984). 70 g of the raw fibres were soaked in distilled water at 10% consistency for 30 min at 70 °C temperature to remove some water-soluble extractives and dewaxed. The dewaxed fibres were pre-treated with equal volume of hydrogen peroxide and sodium hydroxide at the low AP concentration (1.5%: 1.0% w/v H₂O₂: NaOH); medium AP concentrations (2.5%: 2.0% w/v H₂O₂: NaOH), and high AP concentrations (5.0%: 4.0% w/v H₂O₂: NaOH) premix at the solid to liquid ratio 1:10 consistency in a plastic bag and heated in water bath at 70 °C for 60 min. The reacting mixtures in the plastic bag were regularly kneaded to ensure proper mixing and reaction. The alkaline peroxide treated biomass specimens were subjected to wet mechanical refining using a Sprout-Bauer refiner, and screened. Handsheets formed were subjected to drying in an air conditioned room with a relative humidity (RH) of 50% ± 2.0% and temperature of 23°C ± 1.0°C for 24 hours (inside an air-conditioned room). The yield was determined as the percentage of the pulp dried weight to the original oven dried weight of the biomass, while the kappa number (K_n) and the Canadian standard freeness test CSF were determined according to TAPPI test method T 236 om-85 and T 227 respectively. The kappa number was used to determine the residual lignin in the pulp ($K_n \times 0.15$). The handsheet preparations and the determination of the paper properties were conducted by the TAPPI standard test methods (TAPPI 1997). These include handsheet preparation (T205 – om 95), Thickness (T411 – om 89), and grammage. The mechanical testing of the hand sheets included: Tensile strength (T494), Burst strength (T403 - cm 91), and Tear strength (T414 - cm) in five replicates.

Cellulose Characterization

The cellulose was characterised by the thermal analysis, spectral analysis, microscopic analysis, and fibre crystallisation analysis.

Thermogravimetric analysis TGA

The total weight loss and thermal stability of the fibre samples were evaluated with the aid of Perkin Elmer Perkin Elmer Pyris 1 thermogravimetric analyser TGA-DTG instrument used to determine of the extracted cellulose. 10 mg of the dried OPF sample was heated from 28 °C to 700 °C under a nitrogen atmosphere (40 mL/min) to prevent any their oxidative degradation. The derivative thermogravimetry DTG data was also obtained from the analysis.

Spectroscopic Study by Fourier Transform Infrared FTIR spectra

The FTIR spectra of vascular bundle cellulose fibres were verified using a Thermo Scientific model Nicolet Avatar 360 ESP FT-IR spectrometer. Dried powders of the vascular bundle cellulose were pelletized by mixing the sample with KBr. The pelletized sample was then run on the Infrared spectrometer in the range from 400 to 4000 cm^{-1} .

Scanning Electronic Microscopy SEM examination

Surface Morphological examination of the isolated fibres was carried out using scanning electron microscopy. About 0.01 mg of fiber material was sprinkled on a small cube shape on a stub using tape followed by thin layer gold coating with the aid of a Polaron SC515 SEM coating system (Fisons Instrument). Mounted on SEM stubs using ZEISS EVO MA 10 Scanning Electron Microscopy for the SEM examination.

X-Ray diffractometry analysis XRD

The X-ray diffraction XRD analysis was performed in a Kristalloflex D-5000 X-ray diffraction system (Siemens, Germany) with $\text{CuK}\alpha$ radiation ($\lambda = 1.5406 \text{ \AA}$) generated at a voltage of 40 kV and current of 40 mA was used to characterise the crystalline structure of the isolated fibres. All samples were scanned from 0 to 60° 2θ with a Ni filter to give a monochromatic $\text{Cu-K}\alpha$ radiation ($k = 1.5418 \text{ \AA}$). The crystallinity index (CrI) was calculated using Eq. 1, proposed by Segal *et al.* (1959),

$$\text{CrI} = \frac{I_{002} - I_{am}}{I_{002}} \times 100 \quad (1)$$

where CrI expresses the relative degree of crystallinity, I_{002} is the maximum intensity of the principal peak (002) lattice diffraction representing both crystalline and amorphous regions, while I_{am} is the minimum intensity of diffraction representing only the amorphous part (Neto *et al.* 2013).

Statistical analysis

One way analysis of variance ANOVA was used to characterise the AP pre-treatment on the pulp and paper properties obtained. The multiple comparisons of the mean differences in the AP pre-treatment were evaluated using Duncan's Multiple Range Test (DMRT).

RESULTS AND DISCUSSION

Characterization of AP Pulp Fibre

Morphology characteristics of alkaline peroxide extracted OPF fibres

The SEM images (Fig. 1) provide evidence on changes in the fibre morphology as a result of the alkaline peroxide treatments at different concentrations. The SEM at 1000x magnification (Fig.1) showed the removal of the non-cellulosic matters in the raw fibre after the alkaline peroxide treatment at various concentrations. From Fig. 1a, the surfaces of the raw fibre was characterised by silica craters and bounded fibres that gradually disappeared with alkaline peroxide treatment. It can be seen in Fig. 1b-1d that the alkaline peroxide treatment was able to separate the vascular bundles fibres into individual fibres, indicating the effective dissolution of adhesive compounds such as hemicelluloses and

lignin. At higher AP concentrations (Fig.1d), the release of individual fibres and the degree of delamination of the cellulose cell wall was more pronounced.

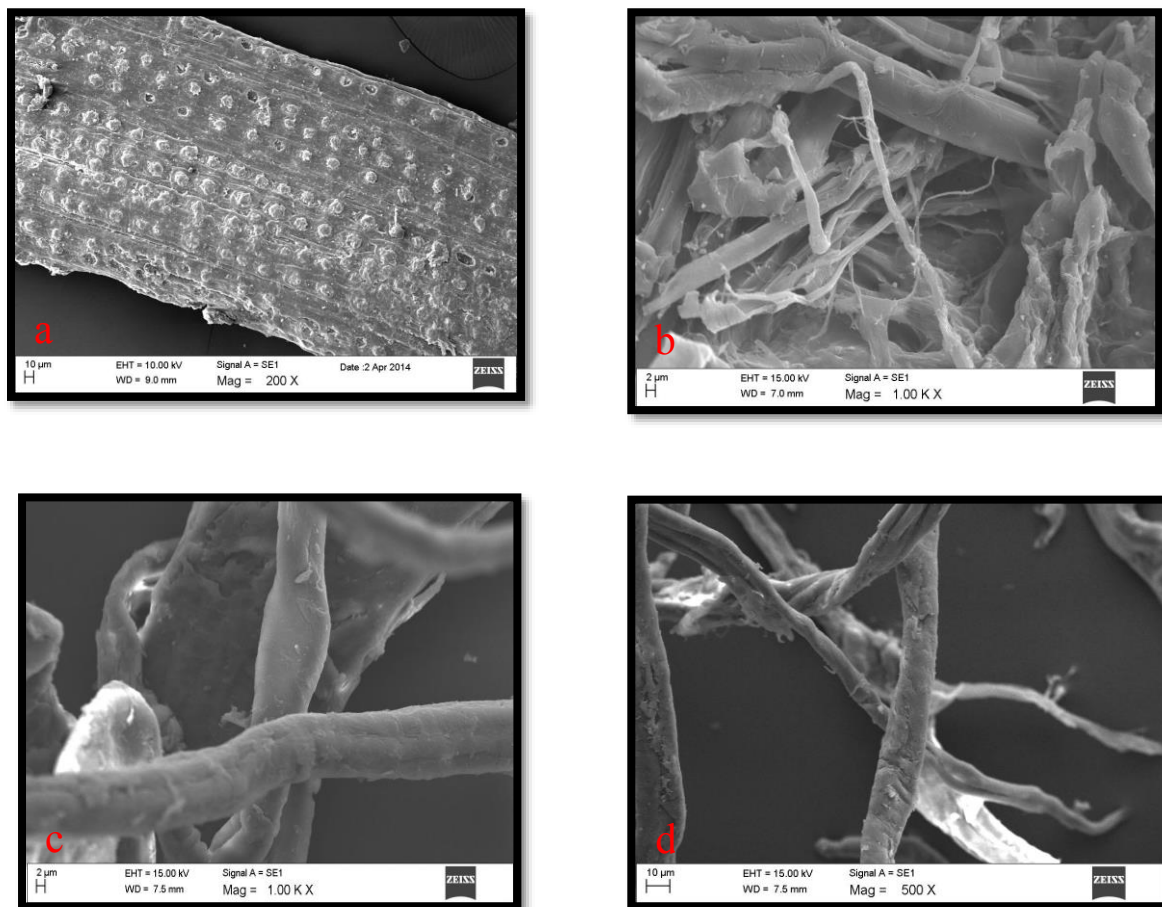


Fig. 1. SEM micrographs of (a) Raw OPF sample; (b) AP fibre extracted at 1.5: 1.0 H₂O₂: NaOH concentrations; (c) AP fibre extracted at 2.5: 2.0 H₂O₂: NaOH concentrations; and (d) AP fibre extracted at 5.0: 4.0 H₂O₂: NaOH concentrations

From the SEM measurement the average fibre diameter of Fig. 1b, Fig. 1c, and Fig.1d were $17.3 \pm 4.12\mu\text{m}$, $10.34 \pm 4.34\mu\text{m}$, and $10.23 \pm 2.91\mu\text{m}$, respectively. Fibres from Fig.1d were characterised by the presence of more fibrillar fines.

Thermogravimetric Analysis (TGA)

From TGA and DTG graphs (Figs. 2 and 3), the initial weight loss was observed to occur between 50 °C and 126 °C for the raw sample, while the weight loss for the extracted samples was observed between 50 °C and 110 °C; 50 °C and 118 °C and 50 °C and 130 °C for cellulose from low; medium, and high AP concentrations, respectively. This first stage of weight loss corresponds to a loss in the volatile materials and vaporisation of water due of the hydrophilic nature of the lignocellulose fibres in all the samples. The second stage of weight loss was observed between 230 °C and 282 °C; 262 °C and 366 °C; 254 °C and 366 °C; and 270 °C and 366 °C for raw and the extracted fibres at low, medium, and high AP concentrations, respectively. This stage corresponded to partial degradation of both

lignin and hemicellulose fractions as a result of the breakdown of ether and carbon–carbon linkages.

From the DTG curves (Fig. 3), the lower temperature peak at around 290 °C was observed for raw (untreated fibre) and AP extracted fibres at H₂O₂:NaOH 1.5:1.0, which corresponded to the decomposition of hemicellulose (Moriana *et al.* 2014; Li *et al.* 2015a; Nagalakshmaiah *et al.* 2016). This temperature peak was found to shift to a higher temperature and remained as a shoulder in AP-treated fibres at H₂O₂: NaOH 2.5:2.0 and H₂O₂: NaOH 5.0:4.0, indicating partial removal of hemicellulose from the fibre. The alkaline peroxide premix was characterised by the generation of intermediate radicals and anions that take part in the depolymerisation of lignin molecule, hence reducing them. Likewise, the near complete absence of hemicellulose in the medium and high AP extracted fibres is attributable to the action of the hydronium ion from water molecule occasioned by the reaction of the intermediate radical and anions from alkaline peroxide premix. This hydronium ion from water molecule catalyses the depolymerization, and subsequently, dissolution of the hemicellulose fraction of lignocellulosic substrate. Depending on the severity of the operational conditions, the oligosaccharides can become further decomposed (Garrote *et al.* 1999). The third decay stage represents thermal degradation peaks around of the samples. From the DTG results shown in Fig 3, the thermal degradation peak corresponded to 342 °C; 366 °C; 374 °C; and 382 °C for untreated OPF raw fibre and cellulose fibres obtained at low, medium, and high AP concentrations respectively, which correspond to the decomposition temperature of cellulose (Yang *et al.* 2010). The results show that there was a significant effect of the AP treatment at different concentrations on the thermal stability of the extracted cellulose fibres. This weight loss was attributed to thermal depolymerization of hemicellulose lignin, pectin, and cleavage of the glycosidic linkages of cellulose (Missoum *et al.* 2013).

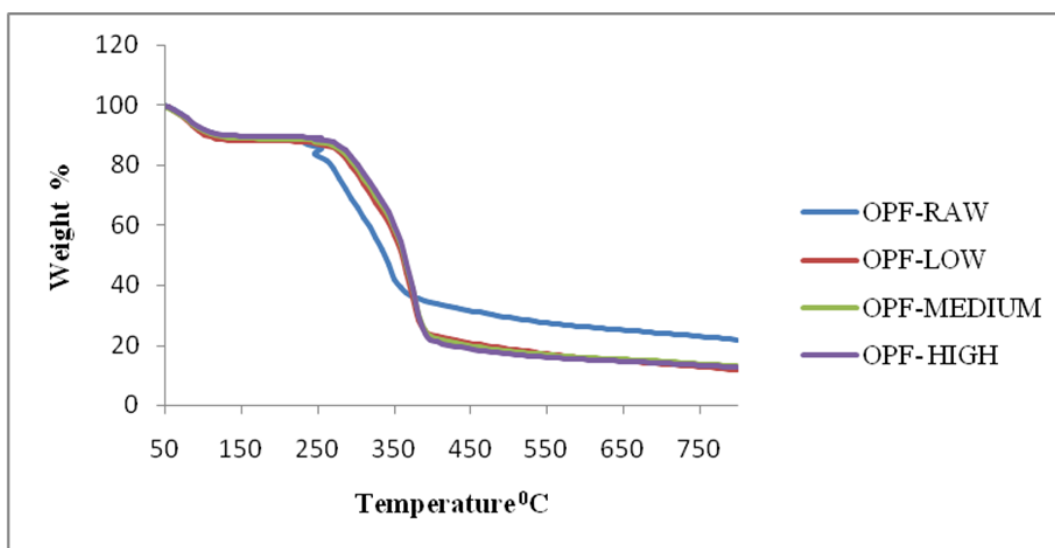


Fig. 2. TG curve of the raw and extracted fibres at different AP concentrations: OPF-RAW, OPF-LOW, OPF-MEDIUM and OPF-HIGH indicates untreated raw OPF fibre, extracted AP fibre at H₂O₂: NaOH (1.5%:1.0%); H₂O₂: NaOH (2.5%:2.0%) and H₂O₂: NaOH (5.0%:4.0%) respectively

From the DTG result, it could be seen that the extracted cellulose fibres had higher thermal stability than the raw OPF fibre. Most wood types commonly used as filler in polymers are processed at temperatures around 200 °C (Moriana *et al.* 2015); high thermal

stability of the alkaline peroxide extracted fibres could be useful alternative as nanofibrous reinforced polymer composites.

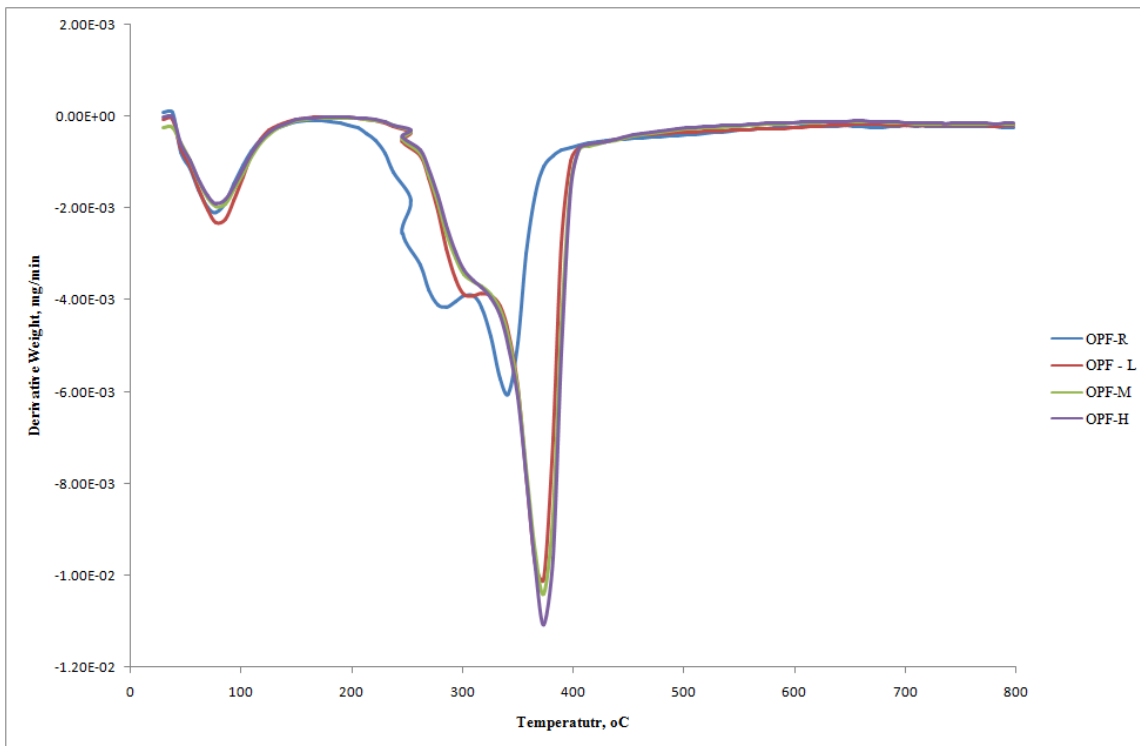


Fig. 3. DTG curve of the raw and extracted fibres at different AP concentrations: OPF-RAW, OPF-LOW, OPF-MEDIUM, and OPF-HIGH indicates untreated raw OPF fibre, extracted AP fibre at H₂O₂: NaOH (1.5%:1.0%); H₂O₂: NaOH (2.5%:2.0%) and H₂O₂: NaOH (5.0%:4.0%) respectively

Due to the high thermal stability of lignin, it is hard to decompose it totally; hence, it is considered to be a major constituent of the residual char (Yang *et al.* 2010; Laurichesse and Avérous 2014).

The amount of residual lignin could be estimated by the quantity of the residual char after the TGA analysis. From the result of this study, the residual char levels of 27.47%; 12.71%; 13.55%, and 13.34% were obtained for untreated OPF fibre and cellulose fibres obtained at low, medium, and high AP concentrations, respectively.

X-Ray diffraction (XRD)

To determine the effect of the AP pre-treatment on the fibres crystallinity, the XRD of the AP pre-treated fibres were examined. The X-ray diffraction patterns of extracted cellulose at different AP concentrations are shown in Fig. 4. The diffraction patterns depict a typical semi-crystalline cellulose fibre material with a mixture of amorphous broad bumps and crystalline peaks.

It is evident from Fig. 4 that the peaks at 22.20°, 22.40°, and 22.10° corresponded to AP extracted fibres: A, B, and C, respectively, are a characteristic pattern of native cellulose, typical of the cellulose I polymorph (Segal *et al.* 1959). This provides evidence that the original crystalline structure of cellulose (cellulose I) was not affected by the alkaline peroxide pre-treatment.

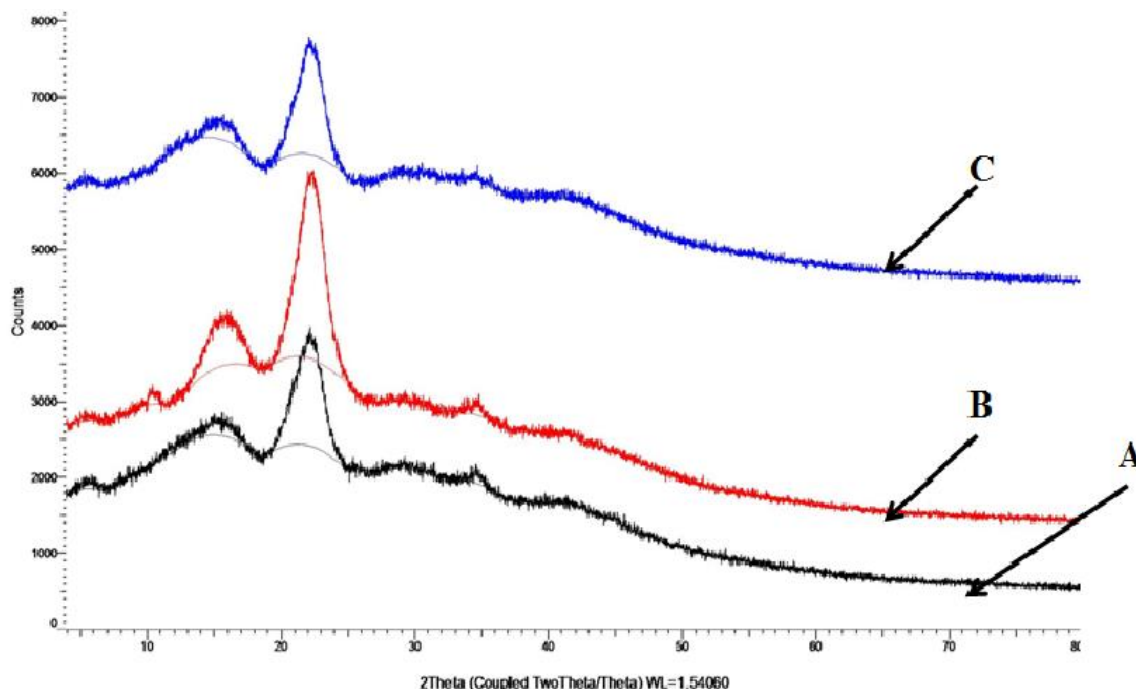


Fig. 4. X-ray diffractometry patterns of AP extracted fibre at (A) 1.5%:1.0%; H₂O₂:NaOH AP concentrations (B) OPF isolated at 2.5%:2.0%; H₂O₂:NaOH AP concentrations (C) OPF isolated at 5.0%:4.0%; H₂O₂:NaOH AP concentrations

It has been reported that cellulose is partly crystalline and partly amorphous in molecular structure, meaning that the cellulose chains contains the crystalline (ordered) regions and the amorphous (disordered) regions (Moriana *et al.* 2014; Nagalakshmaiah *et al.* 2016).

The percentage crystallinity CrI was calculated from Segal equation (Eq. 1), where the diffraction planes of $2\Theta = 22.36^\circ$ was taken as crystalline phase and $2\Theta = 19.31$ as an amorphous phase. There was an increase in the cellulose crystallinity from 28.1% for cellulose obtained from 1.5%:1.0%; H₂O₂: NaOH AP concentrations to 35.7% for cellulose fibre extracted at 2.5%:2.0%; H₂O₂ AP concentrations. This increment is attributable to the ability of the alkaline peroxide to dissolve some of the non-cellulosic parts of the biomass that are mainly amorphous based. However, a decrease in the crystallinity of the fibre to 27.4% was observed from cellulose fibre as the alkaline peroxide concentrations were increased to 5.0%:4.0%; H₂O₂: NaOH.

The observed drop in the percentage crystallinity of the extracted fibre at high AP concentrations was as a result of a high degree of refining of the treated fibre, giving rise to fines-rich fibre produced at high AP concentration. Segal *et al.* (1959) observed that prolonged refining of crystalline cellulose resulted in the almost complete disappearance of substrate's crystallinity. Similarly, both Chauhan and Chakrabarti (2011) and Lamaming *et al.* (2015) independently reported changes in crystallinity index of the respective substrate due to pretreatment. Li *et al.* (2012) opined that during refining, the intermolecular hydrogen bonds of cellulose are broken, causing the collapse of the crystal structure of the cellulose fibre. The X-ray diffraction technique revealed that the extracted cellulose fibres could be easily hydrolyzed into the crystalline sample.

Correlation between Fourier Transform Infrared Spectroscopy FTIR, DTG, and XRD

The result of the FTIR spectroscopy carried out on untreated OPF fibres and the AP extracted cellulose fibres is shown in Fig. 5. Two regions of the FT-IR spectra (Fig.4), namely broadband- 3409.98 to 3381.45 cm^{-1} region (corresponding to the OH stretching frequencies of cellulose) and 1734.01 to 897.21 cm^{-1} , region (“fingerprint region”, corresponding to the different stretching vibrations of the cellulose groups) were observed. The insignificant shift in the spectra of the aliphatic methylene bands at 2903.79 to 2921.77 cm^{-1} , which can be ascribed to C–H stretching, indicates that the reaction does not involve any degradation process of the cellulosic fibre (Mokhothu and John 2015; Li *et al.* 2015a), reconfirming that the α -cellulose was not significantly degraded by the alkaline peroxide treatment.

The band at 1734 to 1733 cm^{-1} in the spectrum of raw biomass and cellulose extracted at low AP concentration is assigned to either the ester linkage of the carboxylic group or the acetyl and uronic ester groups of the ferulic and p -coumeric acids in an unconjugated carbonyl group typical of the hemicelluloses (Neto *et al.* 2013). This band reduces and remains as a shoulder at the medium and high AP treatment characteristic of hemicelluloses dissolution at the medium and high AP concentrations. This observation is in agreement with the DTG result.

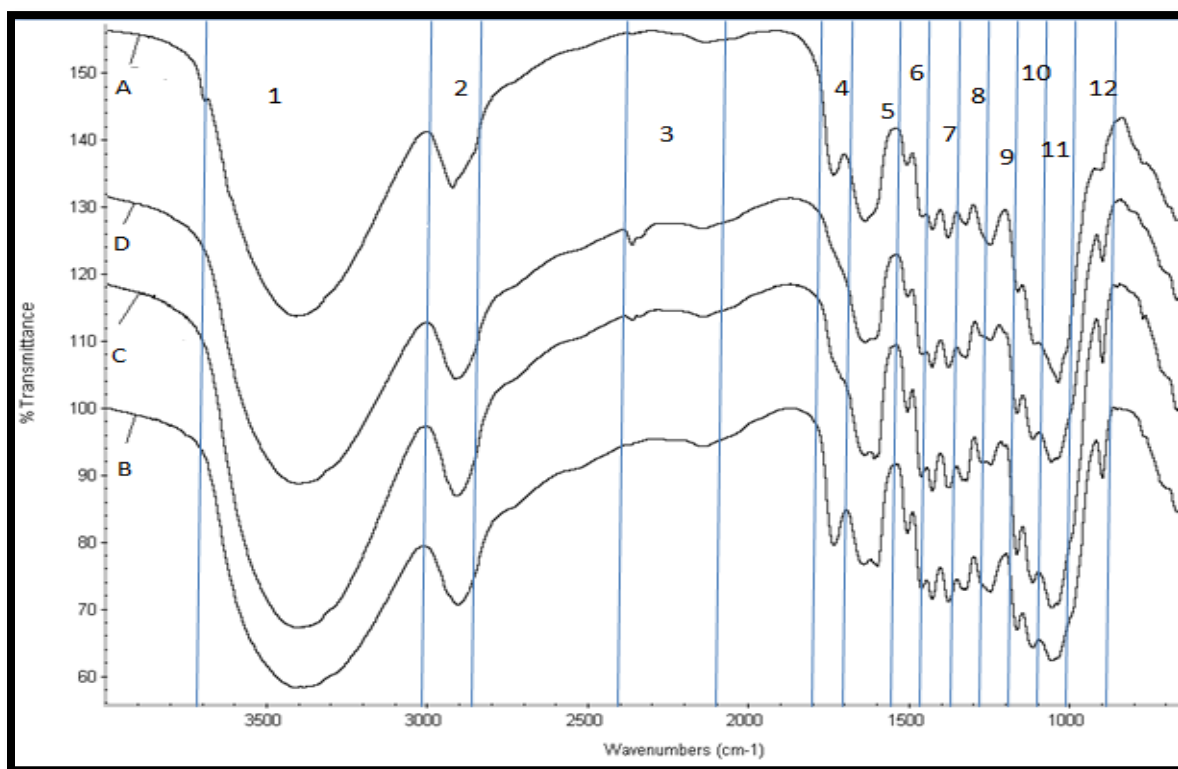


Fig. 5. FTIR spectra of OPF fibre (A) Raw OPF vascular bundles (B) OPF isolated at 1.5%:1.0%; H_2O_2 :NaOH AP concentrations (C) OPF isolated at 2.5%:2.0%; H_2O_2 :NaOH AP concentrations (D) OPF isolated at 5.0%:4.0%; H_2O_2 :NaOH AP concentrations

The dissolution of lignin molecules was evidenced by the shifting in the lignin bands found at 1503 to 1505 cm^{-1} for C=C stretching of the aromatic ring, at 1460 to 1461 cm^{-1} for CH_3 bending, and at 1246 to 1247 cm^{-1} for C=O stretching in lignin (guaiacyl)

molecule (Vanhatalo and Dahl 2014). The slight shift in the peaks at 1640 to 1636 cm^{-1} and the appearance of peak 897 cm^{-1} in the treated fibre indicate stretching vibration of absorbed water in carbohydrates and the C-H deformation vibrations of cellulose, respectively. This information further showed that hemicelluloses and lignin were to a considerable degree dissolved after the alkaline peroxide treatment of the biomass at high AP concentration, while the original molecular structure of the cellulose remained undegraded (Ju *et al.* 2015). Furthermore, bands assigned to cellulose were located at 1426 to 1427 cm^{-1} and 1375 cm^{-1} for CH_2 and C-H bending mode, respectively, at 1163 cm^{-1} and 897 cm^{-1} and at 1320 to 1322 cm^{-1} for CH_2 wagging, distinguished between amorphous and crystallised cellulose (von *et al.* 2014; Wang *et al.* 2013). A shift of the band at 1426 cm^{-1} (assigned to amorphous and crystallised cellulose) to 1427 to 1461 cm^{-1} (characteristic of crystallised cellulose), indicated that the amorphous area of the cellulosic component was more affected by the alkaline peroxide treatment, showing the ease of crystallinity during hydrolysis, as also observed by XRD result (Zakzeski and Weckhuysen 2011). Also, the slightly shift band at 1160 to 1164 cm^{-1} (Fig. 5) shows the vulnerability of the biomass to basic hydrolysis to form cellulose crystals.

Influence of AP Pre-treatment on Pulp and Paper Properties

The Duncan Multiple Range test DMRT was used to find the significant differences in the AP concentration levels for the homogenous subset of all the independent variables distinctions, as denoted by the letters a, b, and c. The results from Table 1 show that the pulp and paper properties increased with an increase in the AP pre-treatment concentration.

Table 1. Duncan Multiple Range Test (DMRT) for the Effect of Alkaline Peroxide Pre-treatment on Pulp and Paper Strength Properties

Treatment	PH	Yield (%)	Kappa Number	CSF (mls.)	Tensile Index (mN/g)	Burst Index (kpam ² /g)	Tear Index (mNm ² /g)
Low	13.45	40.21 ^b	114.55 ^a	780 ^a	1.59 ^c	2.87 ^c	2.33 ^c
Medium	13.70	42.67 ^a	101.10 ^b	550 ^b	9.085 ^b	5.95 ^b	5.37 ^b
High	14.00	38.07 ^c	91.20 ^c	241.67 ^c	13.34 ^a	7.90 ^a	5.63 ^a

In Table 1, ^{a,b,c} are the significant AP pre-treatment levels, with ^a representing the highest, ^b represents mild and ^c representing the least. Treatment. Means within a column with different letters are significantly different at <0.05.

The best treatment was obtained at a high AP concentration for all the mechanical strength properties. The mechanism of alkaline peroxide delignification is based on the formation of hydroperoxy radical ($\bullet\text{OOH}$), hydroxyl radical ($\bullet\text{OH}$), and superoxide anion ($\bullet\text{O}_2$) that are intermediate products of alkaline peroxide premix in the absence of any stabilising agent (Gould 1984, 1985; Liu 2003). These anions and radicals participate in the depolymerisation of both the lignin and the hemicellulose fractions in the lignocellulosic biomass. The decline in the screened pulp yield obtained at high AP concentration is attributable to the high rate of micro-to-nano scale cogenerated fibrils that escaped the R200 screen during screening, hence resulted in low screened pulp yield. The presence of the residual fine particles enhances the water retention of the pulp web, resulting in the low value of the CSF as shown in Table 1 at high AP concentrations. From the qualitative perspective, an increase in alkaline peroxide level is attributable to the better

extent of lignin dissolution. However during paper making, refined, and dignified fibres undergo improved bonding as a result of internal and external fibrillation (Hubbe *et al.* 2007). As a consequence, an increased amount of delignification agents was available to access the more remote chromophoric groups within the rachis structure. This contributed to the low kappa number obtained at high AP concentration. The increased lignin dissolution as the AP concentration increases promotes fibre separations and fibre swelling. This phenomenon contributes to the increase in the inter-fibre bonding and hydrogen bonding and van-der-Waals forces which contributed to the increased mechanical strength properties as the AP concentration increases. From the test, it could be concluded that alkaline peroxide pretreatment is best favoured by mild alkaline peroxide pretreatment (medium concentrations) for paper making pulp and bio-composite production.

CONCLUSIONS

1. The study revealed that alkaline peroxide pretreatment at various AP concentrations produced a high quality of pulp that could be attributed to easier fibre separation.
2. The result showed that there is the possibility of obtaining cellulose fibres that are appropriate for both paper and bio-fillers or as reinforcement in biopolymer composite from alkaline peroxide treated oil palm fronds rachis.
3. The thermal analysis showed that the AP extracted cellulose fibres had higher thermal stability than the raw sample, which made them suitable as biodegradable raw material in the polymer composite.
4. The SEM study showed that the fibres extracted were mainly micro-fibrillated cellulose fibres with an average fibre diameter ranging between $10.23 \pm 2.91\mu\text{m}$ and $17.3 \pm 4.12\mu\text{m}$.
5. The FTIR spectrometry analysis revealed the gradual dissolution of the lignin and hemicellulose as the AP concentrations increased. This result is consistent with results obtained from XRD and TGA analysis.
6. The percentage crystallinity of the extracted cellulose fibres increased with increase in the AP pre-treatment but decreased at high AP concentrations due to the characteristic fine rich fibre formed at high AP treatment.
7. Furthermore, XRD analysis showed a broad peak at the crystalline region with the percentage crystallinity increasing with increase in the AP concentrations. The study showed that these extracted fibres will be useful in paper production and with further processing could be used as raw material for biodegradable nanocomposites with improved qualities.

ACKNOWLEDGMENTS

This research was part of first author's dissertation and financially supported through University Research Grant 1001/PTEKIND/814048, disbursed by Ministry of Science and Technology to Universiti Sains Malaysia.

REFERENCES CITED

- Avolio, R., Graziano, V., Pereira, Y., Cocca, M., Gentile, G., Errico, M., Ambrogi, V., and Avella, M. (2015). "Effect of cellulose structure and morphology on the properties of poly (butylene succinate-co-butylene adipate) biocomposites," *Carbohydrate Polymers* 133, 408-420. DOI: 10.1016/j.carbpol.2015.06.101
- Awalludin, M. F., Sulaiman, O., Hashim, R., and Nadhari, W. N. A. W. (2015). "An overview of the oil palm industry in Malaysia and its waste utilization through thermochemical conversion, specifically via liquefaction," *Renewable and Sustainable Energy Reviews* 50, 1469-1484. DOI: 10.1016/j.rser.2015.05.085
- Borchani, K. E., Carrot, C., and Jaziri, M. (2015). "Untreated and alkali treated fibers from Alfa stem: Effect of alkali treatment on structural, morphological and thermal features," *Cellulose* 22, 1577-1589. DOI: 10.1007/s10570-015-0583-5
- Chauhan, V. S., and Chakrabarti, S. K. (2012). "Use of nanotechnology for high performance cellulosic and papermaking products," *Cellulose Chemistry and Technology* 46, 389-400.
- Daud, W. R. W., Kassim, M. H. M., and Mohamded, M. A. S. (2011). "Cellulose phosphate from oil palm biomass as potential biomaterials," *BioResources* 6, 1719-1740. DOI: 10.15376/biores.6.2.1719-1740
- Fahma, F., Iwamoto, S., Hori, N., Iwata, T., and Takemura, A. (2011). "Effect of pre-acid-hydrolysis treatment on morphology and properties of cellulose nanowhiskers from coconut husk," *Cellulose* 18, 443-450. DOI: 10.1007/s10570-010-9480-0
- French, A. D., and Cintrón, M. S. (2013). "Cellulose polymorphy, crystallite size, and the Segal crystallinity index," *Cellulose* 20, 583-588. DOI: 10.1007/s10570-012-9833-y
- Garrote, G., Dominguez, H., and Parajo, J. C. (1999). "Mild autohydrolysis: An environmentally friendly technology for xylooligosaccharide production from wood," *Journal of Chemical Technology and Biotechnology* 74, 1101-1109. [http://dx.doi.org/10.1002/\(SICI\)1097-4660\(199911\)74:11<1101::AID-JCTB146>3.0.CO;2-M](http://dx.doi.org/10.1002/(SICI)1097-4660(199911)74:11<1101::AID-JCTB146>3.0.CO;2-M)
- Ghazali, A., Zukeri, M., Hafiz, M. R., Wanrosli, W.D., Azhari, B., Ibrahim, R., Ahmed, M. I., Ahmad, T., and Khan, Z. A. (2014). "Augmentation of EFB fiber web by nano-scale fibrous elements," *Advanced Materials Research* 832, 494-499. DOI: 10.4028/www.scientific.net/AMR.832.494
- Gould, J. M. (1984). "Alkaline peroxide delignification of agricultural residues to enhance enzymatic saccharification," *Biotechnology and Bioengineering* 26, 46-52. DOI: 10.1002/bit.260260110
- Gould, J. M. (1985). "Studies on the mechanism of alkaline peroxide delignification of agricultural residues," *Biotechnology and Bioengineering* 27, 225-231. DOI: 10.1002/bit.260270303
- Haafiz, M. M., Eichhorn, S., Hassan, A., and Jawaid, M. (2013). "Isolation and characterization of microcrystalline cellulose from oil palm biomass residue," *Carbohydrate Polymers* 93, 628-634. DOI: 10.1016/j.carbpol.2013.01.035
- Hubbe, M. A., Venditti, R. A., and Rojas, O. J. (2007). "What happens to cellulosic fibers during papermaking and recycling? A review," *BioResources* 2(4), 739-788. DOI: 10.15376/biores.2.4.739-788
- Ju, X., Bowden, M., Brown, E. E., and Zhang, X. (2015). "An improved X-ray diffraction method for cellulose crystallinity measurement," *Carbohydrate Polymers* 123, 476-481. DOI: 10.1016/j.carbpol.2014.12.071

- Khalil, H. A., Hossain, M. S., Rosamah, E., Azli, N., Saddon, N., Davoudpoura, Y., Islam, M. N., and Dungani, R. (2015). "The role of soil properties and its interaction towards quality plant fiber: A review," *Renewable and Sustainable Energy Reviews* 43, 1006-1015. DOI: 10.1016/j.rser.2014.11.099.
- Kwon, H.-J., Sunthornvarabhas, J., Park, J.-W., Lee, J.-H., Kim, H.-J., Piyachomkwan, K., Sriroth, K., and Cho, D. (2014). "Tensile properties of kenaf fiber and corn husk flour reinforced poly (lactic acid) hybrid bio-composites: Role of aspect ratio of natural fibers," *Composites Part B: Engineering* 56, 232-237. DOI: 10.1016/j.compositesb.2013.08.003.
- Lamaming, J., Hashim, R., Leh, C. P., Sulaiman, O., Sugimoto, T., and Nasir, M. (2015). "Isolation and characterization of cellulose nanocrystals from parenchyma and vascular bundle of oil palm trunk (*Elaeis guineensis*)," *Carbohydrate Polymers* 134, 534-540. <http://dx.doi.org/10.1016/j.carbpol.2015.08.017>.
- Laurichesse, S., and Avérous, L. (2014). "Chemical modification of lignins: Towards biobased polymers," *Progress in Polymer Science* 39, 1266-1290. DOI: 10.1016/j.progpolymsci.2013.11.004
- Li, M.-F., Li, X., Bian, J., Chen, C.-Z., Yu, Y.-T., and Sun, R.-C. (2015a). "Effect of temperature and holding time on bamboo torrefaction," *Biomass and Bioenergy* 83, 366-372. DOI: 10.1016/j.biombioe.2015.10.016
- Li, R., Wang, S., Lu, A., and Zhang, L. (2015b). "Dissolution of cellulose from different sources in an NaOH/urea aqueous system at low temperature," *Cellulose* 22, 339-349. DOI: 10.1007/s10570-014-0542-6
- Li, J., Wei, X., Wang, Q., Chen, J., Chang, G., Kong, L., Su, J., and Liu, Y. (2012). "Homogeneous isolation of nanocellulose from sugarcane bagasse by high pressure homogenization," *Carbohydrate Polymers* 90, 1609-1613. DOI: 10.1016/j.carbpol.2012.07.038 PMID:22944423
- Liu, S. (2003). "Chemical kinetics of alkaline peroxide brightening of mechanical pulps," *Chemical Engineering Science* 58, 2229-2244. DOI: 10.1016/S0009-2509(03)00089-7
- Missoum, K., Martoia, F., Belgacem, M. N., and Bras, J. (2013). "Effect of chemically modified nanofibrillated cellulose addition on the properties of fiber-based materials," *Industrial Crops and Products* 48, 98-105. DOI: 10.1016/j.indcrop.2013.04.013
- Mokhothu, T. H., and John, M. J. (2015). "Review on hygroscopic aging of cellulose fibres and their biocomposites," *Carbohydrate Polymers* 131, 337-354. DOI: 10.1016/j.carbpol.2015.06.027
- Moriana, R., Vilaplana, F., and Ek, M. (2015). "Forest residues as renewable resources for bio-based polymeric materials and bioenergy: Chemical composition, structure and thermal properties," *Cellulose* 22, 3409-3423. DOI: 10.1007/s10570-015-0738-4
- Moriana, R., Vilaplana, F., Karlsson, S., and Ribes, A. (2014). "Correlation of chemical, structural and thermal properties of natural fibres for their sustainable exploitation," *Carbohydrate Polymers* 112, 422-431. DOI: 10.1016/j.carbpol.2014.06.009
- Nagalakshmaiah, M., Mortha, G., and Dufresne, A. (2016). "Structural investigation of cellulose nanocrystals extracted from chili leftover and their reinforcement in cariflex-IR rubber latex," *Carbohydrate Polymers* 136, 945-954. DOI: 10.1016/j.carbpol.2015.09.096
- Neto, W. P. F., Silvério, H. A., Dantas, N. O., and Pasquini, D. (2013). "Extraction and characterization of cellulose nanocrystals from agro-industrial residue – soy hulls," *Industrial Crops and Products* 42, 480-488. DOI: 10.1016/j.indcrop.2012.06.041

- Ng, H.-M., Sin, L. T., Tee, T.-T., Bee, S.-T., Hui, D., Low, C.-Y., and Rahmat, A. (2015). "Extraction of cellulose nanocrystals from plant sources for application as reinforcing agent in polymers," *Composites Part B: Engineering* 75, 176-200. DOI: 10.1016/j.compositesb.2015.01.008
- Segal, L., Creely, J., Martin, A., and Conrad, C. (1959). "An empirical method for estimating the degree of crystallinity of native cellulose using the X-ray diffractometer," *Textile Research Journal* 29, 786-794. DOI: 10.1177/004051755902901003
- Silvério, H. A., Neto, W. P. F., Dantas, N. O., and Pasquini, D. (2013). "Extraction and characterization of cellulose nanocrystals from corncob for application as reinforcing agent in nanocomposites," *Industrial Crops and Products* 44, 427-436. DOI: 10.1016/j.indcrop.2012.10.014
- Vanhatalo, K. M., and Dahl, O. P. (2014). "Effect of mild acid hydrolysis parameters on properties of microcrystalline cellulose," *BioResources* 9, 4729-4740. DOI: 10.15376/biores.9.3.4729-4740
- Wang, K., Yang, H., Chen, Q., and Sun, R.-C. (2013). "Influence of delignification efficiency with alkaline peroxide on the digestibility of furfural residues for bioethanol production," *Bioresource Technology* 146, 208-214. DOI: 10.1016/j.biortech.2013.07.008
- Wanrosli, W., Rohaizu, R., and Ghazali, A. (2011). "Synthesis and characterization of cellulose phosphate from oil palm empty fruit bunches microcrystalline cellulose," *Carbohydrate Polymers* 84, 262-267. DOI: 10.1016/j.carbpol.2010.11.032
- Wanrosli, W., Zainuddin, Z., Law, K., and Asro, R. (2007). "Pulp from oil palm fronds by chemical processes," *Industrial Crops and Products* 25, 89-94. DOI: 10.1016/j.indcrop.2006.07.005
- Yang, Q., Lue, A., and Zhang, L. (2010). "Reinforcement of ramie fibers on regenerated cellulose films," *Composites Science and Technology* 70, 2319-2324. DOI: 10.1016/j.compscitech.2010.09.012
- Zakzeski, J., and Weckhuysen, B. M. (2011). "Lignin solubilization and aqueous phase reforming for the production of aromatic chemicals and hydrogen," *ChemSusChem* 4, 369-378. DOI: 10.1002/cssc.201000299
- Zhang, T., Guo, M., Cheng, L., and Li, X. (2015). "Investigations on the structure and properties of palm leaf sheath fiber," *Cellulose* 22, 1039-1051. DOI: 10.1007/s10570-015-0570-x

Article submitted: December 24, 2015; Peer review completed: January 23, 2016;
Revised version received: January 29, 2016; Accepted: January 30, 2016; Published:
February 4, 2016.

DOI: 10.15376/biores.11.2.3013-3026